

Orientation of axes in the elbow and forearm for biomechanical modeling

DirkJan (H.E.J.) Veeger, Bing Yu*, Kai Nan An*

*Institute for Fundamental and Clinical Human Movement Sciences,
Institute for Fundamental and Clinical Human Movement Sciences, Department of Human Movement
Sciences, Vrije Universiteit, Amsterdam, the Netherlands

*Orthopedic Biomechanics Laboratory, Mayo Clinic, Rochester MN, USA

ABSTRACT - To extend an already existing three-dimensional (3-D) model of the shoulder (Van der Helm, 1994) a cadaver study was performed in which quantitative information on the 3-D orientations of rotation axes in the upper extremity was collected.

To calculate axes, we measured the glenohumeral, humeroulnar and ulnoradial movements on five human cadaver arms (four right arms, one left). Movement was measured with an electromagnetic tracking system which sensors were directly attached to scapula, humerus, ulna and radius. In addition, a series of anatomical landmarks was measured. From the tracking data, the Instantaneous Helical Axes (IHA) were calculated, as well as the resulting optimal mean Gleno-Humeral (GH) center of rotation, Flexion-Extension (FE) axis and Pronation-Supination (PS) axis. To allow for the construction of a musculoskeletal model, anatomical landmarks, were transformed from the global measurement co-ordinate system to separate local co-ordinate systems, related to the rotation center and axes of rotation.

The FE- and PS-axis could be determined accurately and were found to be almost perpendicular ($88.9 \pm 5.1^\circ$) and crossed at 3.3 ± 0.8 mm.

It is suggested that forearm movements can be modelled with a two Degree-of-Freedom model.

INTRODUCTION

Biomechanical modeling of the upper extremity can play an important role in understanding the causes of upper extremity disorders and the corresponding treatment. Also, a biomechanical model can be used to get insight into more fundamental issues on motor control. Recently, a three-dimensional (3-D) model of the shoulder has been developed (Van der Helm, 1994). This model is based on morphological data that were collected in an extensive cadaver study (Veeger et al, 1991). However, this cadaver study did not embrace data for extension of the model to the elbow and the elbow function had to be modeled with a three Degree-of-Freedom (DOF) joint (Van der Helm, 1994). To improve the range of the model and to allow for more accurate modeling of the function of the bi-articular arm muscles, the addition of a morphologically more realistic description of the arm was judged to be necessary. Since previous studies generally reported qualitative descriptions of elbow flexion axes (Fick, 1911; Morrey & Chao, 1976; Deland et al, 1987; Youm et al, 1979) and forearm pro-supination axes (Fick, 1911; Morrey & Chao 1976; Hollister et al, 1994) those data were not available from the literature.

The aim of this project was to collect quantitative information on the 3-D orientations of the rotation center and axes of rotation in the upper extremity.

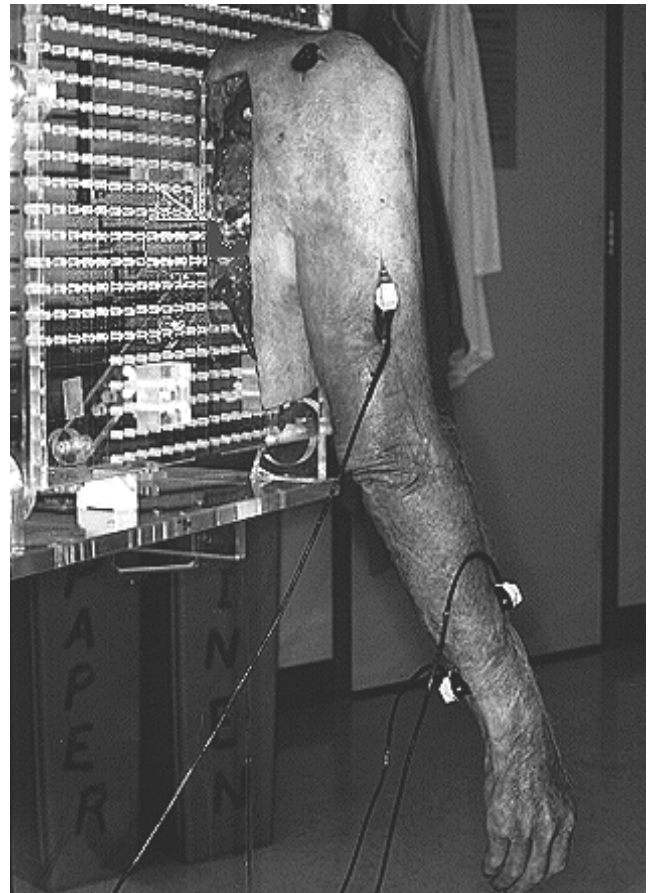


Figure 1-Illustration of the experimental set-up and positioning of sensors.

Table 1- Description of definitions of local co-ordinate systems for scapula, humerus, ulna and radius.

Segment	Axis	Definition	Relevant landmarks
Scapula	X-axis	pointing from AC to TS	AC = dorsal point on the AcromioClavicular joint TS = Trigonum Spinae AI = Angulus Inferior AA = Angulus Acromialis PC = Processus Coracoideus
	Z-axis	perpendicular to AC - TS - AI, pointing backwards	
	Y-axis origin	perpendicular to X and Z AC	
Humerus	Y-axis	pointing from MP to GH	GH = Glenohumeral Rotation Center EM = Epicondylus Medialis EL= Epicondylus Lateralis MP = midpoint between EM and EL
	Z-axis	perpendicular to GH - EM - EL, pointing backwards	
	X-axis origin	perpendicular to Y and Z GH	
Ulna	X-axis	along the FE-axis	US = Processus Styloideus Ulnae OL = Olecranon
	Z-axis	perpendicular to the plane formed by US and the FE-axis, pointing backwards	
	Y-axis origin	perpendicular to X and Z point on the FE-axis	
Radius	X-axis	along the PS-axis	RS = Processus Styloideus Radii
	Z-axis	perpendicular to the plane formed by RS and the PS-axis, pointing backwards	
	Y-axis origin	perpendicular to X and Z point on the PS-axis	

METHODS

Five upper extremities were harvested from four fresh specimen at the level of the scapula (four right, one left). This left the scapulohumeral muscles and all more distal structures intact. All four specimen were male, with a mean age, weight and size of 68.5 yr, 80.0 kg and 1.78 m, respectively. The extremities were fastened onto a measuring table in such a way that the scapula was fixed and the arm was fully free to move. Following fixation of 3-D electromagnetic sensors (Isotrack, Polhemus) on scapula, humerus, ulna and radius, the positions of local anatomical landmarks were digitized with an extra sensor, mounted with a stylus (Figure 1). At a later stage the anatomical landmarks were used for the definition of local orientation axes. Subsequently, each arm was moved through a selection of standard directions (glenohumeral ab-adduction, flexion-extension and endo-exorotation, elbow flexion-extension and forearm pro-supination), during which the positions and orientations of each sensor were collected. A typical movement consisted of two cycles in which a joint was moved through its full range of motion. The sampling period was 15 seconds with a sampling frequency of $F_s=10\text{Hz}$.

Sensor data were used to determine the Gleno-Humeral (GH) rotation center and the Flexion-Extension (FE) and Pro-Supination axes. Estimations of the rotation axes were based on the Instantaneous Helical Axes (IHA) algorithms [8]. Prior to calculation of the IHA, the position and angle time series for each sensor were filtered with a cut-off frequency of 1.5 Hz. The angular velocity of each sensor was calculated using the method described by Woltring (1990, 1991):

$$\begin{aligned} \omega_t &= \sqrt{\underline{\omega}^T \underline{\omega}} = |\underline{\omega}_t| \\ \underline{v}_t &= \underline{\omega}_t / \omega_t \\ \underline{s}_t &= \underline{p}_t + \underline{\omega}_t * \dot{\underline{p}}_t / \omega_t^2 \end{aligned} \tag{Eq. 1}$$

where:

- $\underline{\omega}$ = relative angular velocity of the sensor on the distal segment ;
- \underline{p} = relative position of the sensor on the distal segment ;
- \underline{v} = direction vector of the IHA ;
- \underline{s} = projection of \underline{p} on the IHA.

The IHA was calculated for each time sample where the angular velocity of the distal segment, relative to the proximal segment was larger than $0.25 \text{ rad}\cdot\text{s}^{-1}$. To determine a mean helical axis and pivot, the optimal pivot point was calculated as \underline{s}_{opt} , as the mean 'pivot', closest to all Instantaneous Helical Axes in a least-squared sense (Woltring, 1991):

$$\underline{s}_{opt} = Q^{-1} \cdot \frac{1}{n} \cdot \sum_{i=1}^n Q_i \cdot \underline{s}_i \tag{Eq. 2}$$

where:

$$Q_i = (I - \underline{v}_i \cdot \underline{v}_i^T)$$

$$Q = \frac{1}{n} \cdot \sum_{i=1}^n Q_i \tag{Eq. 3}$$

Analogous to the position vector, the optimal direction vector \underline{v}_{opt} was calculated as the vector with the smallest angle between axes.

For each specimen, landmarks and axes were expressed relative to a local co-ordinate system. Table 1 gives an overview of the definitions.

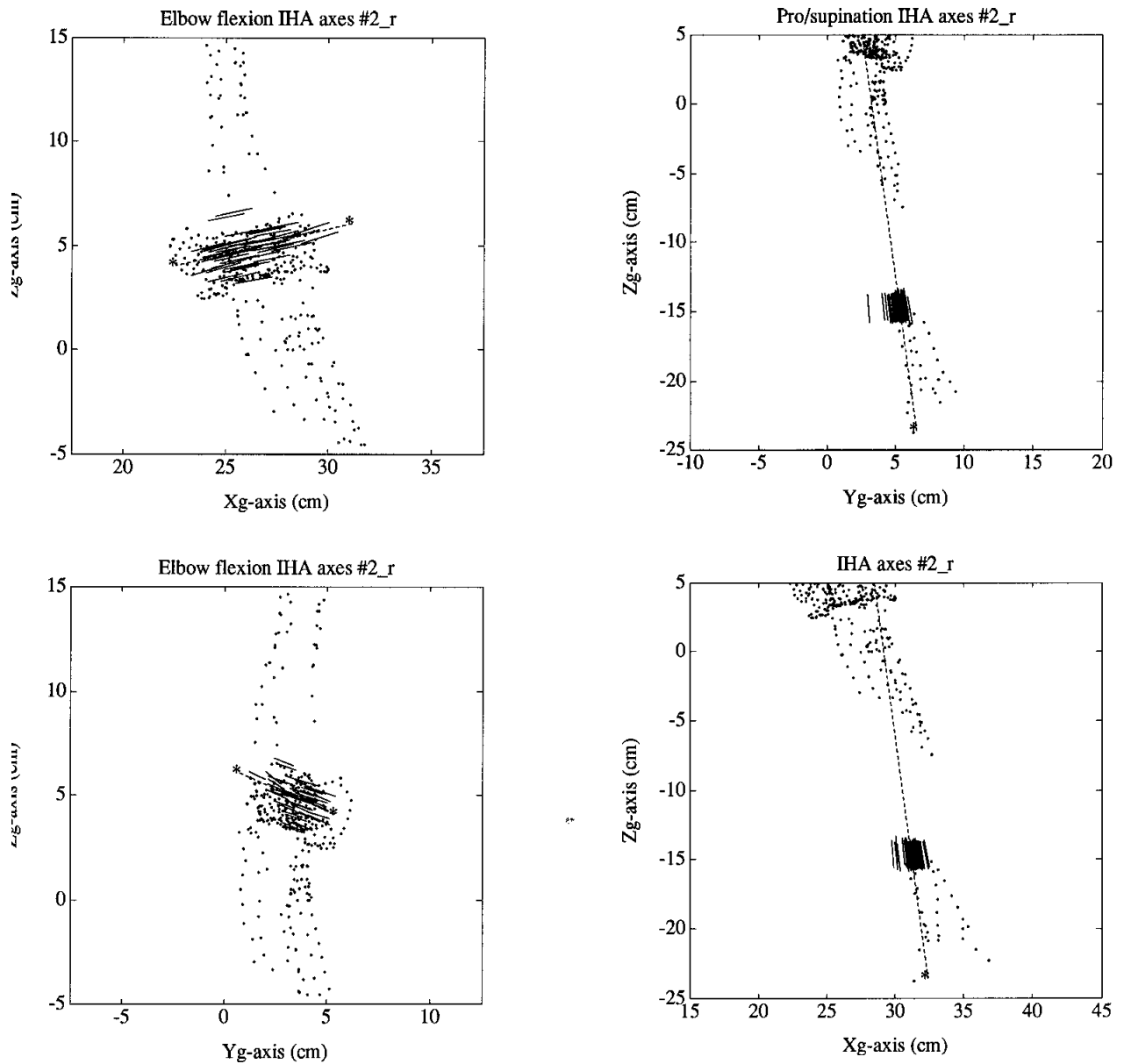


Figure 2- Typical example for IHA calculations for FE and PS, represented in the measurement coordinate system. The X-Z plane roughly corresponds with the frontal plane. IHA are drawn with a length of 2 cm. Dots are data samples from the surfaces of humerus, ulna and radius. The dashed line is the mean IHA.

Table 2- XYZ-coordinates for anatomical landmarks on the scapula. Coordinates are expressed in a local coordinate system in which the AcromioClavicular joint (AC) is chosen as the origin (0, 0, 0). Values are given in cm.

Scapula	Trigonum Spinae	Angulus Inferior	Angulus Acromialis	Processus Coracoideus	GH Rotation Center
k1_r	13.9 0.0 0.0	17.3 12.3 0.0	-0.9 1.5 1.2	2.1 0.3 -3.4	1.0 4.6 -0.3
k2_r	13.5 0.0 0.0	16.8 13.0 0.0	0.2 1.0 3.4	1.2 1.6 -3.8	0.3 3.4 1.0
k3_r	12.1 0.0 0.0	14.6 13.6 0.0	-0.7 -0.0 2.9	1.3 2.3 -3.5	0.2 3.2 0.6
k4_r	13.1 0.0 0.0	16.5 13.7 0.0	0.9 1.1 3.4	1.5 1.6 -4.2	0.8 4.6 -0.8
k2_l	13.5 0.0 0.0	16.7 13.4 0.0	-0.1 0.9 2.7	1.7 2.9 -4.2	0.6 3.9 0.4
mean	13.2 0.0 0.0	16.4 13.2 0.0	-0.1 0.9 2.7	1.5 1.7 -3.8	0.6 3.9 0.2
std	0.7 0.0 0.0	1.0 0.6 0.0	0.7 0.6 0.9	0.4 1.0 0.4	0.3 0.7 0.7

RESULTS AND DISCUSSION

Figure 2 illustrates the helical axes as determined for elbow flexion and forearm pronation. The data are plotted in the measuring co-ordinate system. IHA calculations showed fluctuations in position, but not as much in orientation. The range in individual estimation errors for GH was 0.8 - 1.7 cm. For FE and PS, the mean axes fluctuated most in their direction. For FE, the direction vector was less stable than for PS. The range of estimation errors was 1.5° - 2.6° for FE and 0.4° - 1.2° for PS

The anatomical landmarks and GH rotation center are given in Table 2. The anatomical landmarks are expressed in the local scapula co-ordinate system with the origin in AC. The standard deviation in the GH rotation center is low. The consistency in the relationship between the co-ordinates of the scapular landmarks and the GH-rotation center suggest that the GH center can be predicted from the scapular anatomical landmarks. This supports results by Meskers et al (1996) who predicted the center of the Glenoid from scapular landmarks. With the help of the relationship between scapular landmarks and GH, it will be possible to estimate the position of the rotation center of the GH joint in-vivo which can be used for the definition of the proximal landmark of the humerus.

The anatomical landmarks on the humerus, ulna and radius have been expressed relative to their proximal rotation center and axes (Table 3). Due to the fact that anatomical landmarks on the radius are generally difficult to measure in-vivo, only the co-ordinates for RS are given.

Analysis of the direction and position of the FE- and PS axes indicate that the FE axis does not run parallel to the line EM-EL, but deviates $6.0 \pm 2.6^\circ$ from this line. The orientation of the estimated FE-axis confirms previous qualitative observations that describe a flexion-extension axis as running through the center of the trochlea and the capitulum humeri (Fick, 1911; Morrey & Chao, 1976; Youm et al, 1979; Deland et al, 1987). The suggestion by Morrey and Chao (1976) that the position of the axis is dependent on elbow angle, could not be confirmed. It thus seems reasonable to model the humeroulnar joint as a uniaxial joint.

The PS-axis runs through the radial head and lies close to the anatomical landmarks EL (distance = 13.1 ± 2.2 mm) and US (distance = 8.0 ± 4.5 mm). The average distance to the center of the radial head was found to be 3.2 ± 4.0 mm. Also, the results for the PS-axis confirm earlier descriptions (Fick, 1911; Morrey & Chao, 1976; Hollister et al, 1994) of an orientation of that axis through the center of the radial head and the most distal point on the ulna (which is approximated by US).

The PS-axis crosses the FE-axis at 3.3 ± 0.8 mm and an angle of $88.9 \pm 5.1^\circ$. Given the general uncertainties and input errors in musculoskeletal modeling, it can be concluded that the elbow can be modeled as a system with two kinematic Degrees-of-Freedom.

The results of this study are being implemented in a model of the shoulder and arm. First results indicate a good fit between in-vivo measured arm movements during wheelchair propulsion and kinematic model simulations.

Table 3 - XYZ-coordinates for anatomical landmarks on the humerus, ulna and radius. Coordinates are expressed in local coordinate system in with GH, and points on the FE- and PS-axes as respective origins (0, 0, 0). Values are given in cm.

	Medial Epicondyle	Lateral Epicondyle	Point on FE-axis	Direction of FE-axis
k1_r	-3.5 -29.0 0.0	3.5 -28.7 0.0	0.0 -29.4 -1.1	0.9983 0.0385 0.0445
k2_r	-3.5 -33.1 0.0	3.5 -32.7 0.0	1.3 -33.1 -0.8	0.9817 0.1805 0.0610
k3_r	-3.6 -29.0 0.0	3.6 -29.1 0.0	0.7 -29.8 -0.4	0.9985 0.0476 0.0275
k4_r	-3.6 -31.2 0.0	3.6 -31.6 0.0	1.1 -31.8 -0.8	0.9917 0.0309 -0.1251
k2_l	-3.6 -32.2 0.0	3.6 -31.8 0.0	-1.1 -32.8 -0.9	0.9887 0.1247 0.0837
mean	-3.6 -30.9 0.0	3.6 -30.8 0.0	0.4 -31.4 -0.81	0.9918 0.0844 0.0183
std	0.1 1.9 0.0	0.1 1.8 0.0	1.0 1.7 0.28	0.0070 0.0655 0.0828
Ulna	Ulnar Styloid	Olecranon	Point on PS-axis	Direction of PS-axis
k1_r	3.0 26.2 0.0	-1.3 -1.0 -2.7	2.6 7.2 -0.0	0.0468 0.9977 0.0486
k2_r	-2.5 27.0 0.0	-2.0 -0.5 -3.3	1.0 4.5 0.3	-0.1445 0.9894 0.0115
k3_r	1.4 25.1 0.0	-0.8 -0.8 -2.9	1.7 11.0 -0.2	-0.0106 0.9999 0.0121
k4_r	3.2 27.4 0.0	-2.8 -1.7 -3.0	1.8 10.3 0.1	0.0745 0.9960 0.0488
k2_l	0.5 27.6 0.0	0.4 -0.8 -3.0	3.3 4.3 0.3	-0.0643 0.9978 -0.0127
mean	1.1 26.7 0.0	-1.3 -1.0 -3.0	2.1 7.5 0.1	-0.0196 0.9962 0.0216
std	2.3 1.1 0.0	1.2 0.4 0.2	0.9 3.1 0.2	0.0879 0.0040 0.0266
Radius	Radial Styloid			
k1_r	4.8 17.9 0			
k2_r	4.1 23.7 0			
k3_r	4.2 14.9 0			
k4_r	4.4 17.2 0			
k2_l	4.1 24.2 0			
mean	4.3 19.6 0			
std	0.3 4.2 0			

ACKNOWLEDGMENT

This study was partially supported by a NATO Science Fellowship awarded by the Netherlands Organization for Scientific Research and NIH Grants HD07447 and AR41171.

REFERENCES

Deland J.T., A. Garg, P.S .Walker (1987) Biomechanical basis for elbow hinge-distractor design. *Clin. Orthop. Rel. Res.* 215; 303-312.
 Fick R., (1911) *Handbuch der Anatomie und Mechanik der Gelenke*. Jena: Gustav Fischer.
 Helm F.C.T. Van der, (1994) A finite element musculoskeletal model of the shoulder mechanism. *J. Biomech.* 27(5); 551-570.
 Hollister A.M., H. Gellman, R.L. Waters (1994) The relationship of the interosseous membrane to the axis of rotation of the forearm. *Clin. Orth. Rel. Res.* 298; 272-276.
 Meskers C.G.M., F.C.T. van der Helm, L.A. Rozendaal, P.M. Rozing (1997) Estimation of the glenohumeral joint rotation center from scapula bony landmarks by

linear regression, a cadaver study. In: H.E.J. Veeger, F.C.T. van der Helm, P.M. Rozing (eds.). *Abstracts for the First Conference of the International Shoulder Group*, 26 and 27 August 1996, Delft University of Technology, Delft, The Netherlands.
 Morrey B.F., E.Y.S. Chao (1976) Passive motion of the elbow joint. *J. Bone Joint Surg.* 58-A; 501-508.
 Veeger H.E.J., F.C.T. van der Helm, L.H.V. van der Woude, G.M. Pronk, R.H. Rozendal (1991) Inertia and muscle contraction parameters for musculoskeletal modelling of the shoulder mechanism. *J. Biomech.* 24(7); 615-629.
 Woltring H.J. (1990) Data processing and error analysis. In: *Biomechanics of human movement: Applications in Rehabilitation, Sport and Ergonomics*. (Edited by Capozzo, A and Berme P.) 10.1, pp 203-237.
 Woltring H.J. (1991) Definition and Calculus of Attitude Angles and Instantaneous Helical Axes from noisy Position and Attitude data. In: *Proc. on the Int. Symp. on 3-D Analysis of human Movement*, Montreal, 59-62.
 Youm Y., R.F. Dryer, K. Thambyrajah, A.E. Flatt, B.L. Sprague (1979) Biomechanical analyses of forearm pronation-supination and elbow flexion-extension. *J. Biomech.* 12; 245-255.

